Acta Oceanol. Sin., 2019, Vol. 38, No. 1, P. 151–159
https://doi.org/10.1007/s13131-018-1259-4
http://www.hyxb.org.cn
E-mail: hyxbe@263.net

Response of size-fractionated phytoplankton to environmental factors near the Changjiang Estuary

Li Li[1, 2], Jingyi Cen[1, 2], Lei Cui[1, 2], Songhui Lu[1, 2*]

[1] Research Center for Harmful Algae and Marine Biology, Jinan University, Guangzhou 510632, China

[2] Key Laboratory of Eutrophication and Red Tide Prevention of Guangdong Higher Education Institutes, Jinan University, Guangzhou 510632, China

Received 19 October 2017; accepted 6 February 2018

Abstract

Size-based partitioning of phytoplankton is a useful tool for monitoring key phytoplankton traits, and it provides a better understanding of phytoplankton dynamics. Our aim is to determine the variation in the different size classes of phytoplankton to the total phytoplankton biomass during the spring and autumn of 2010 and examine the relationship between phytoplankton size structure and environmental variables and zooplankton community structure near the Changjiang Estuary. In the spring, phytoplankton populations were predominantly consisted of nanophytoplankton throughout the study region. In the autumn, picophytoplankton and nanophytoplankton collectively dominated the phytoplankton community. A Pearson correlation analysis highlighted the role of temperature and trophic conditions on the contributions of nanophytoplankton and picophytoplankton. The grazing pressure exerted by mesozooplankton could have played an important role in determining the microphytoplankton community structure.

Key words: phytoplankton size structure, temperature, trophic condition, seasonal succession, Changjiang Estuary

Citation: Li Li, Cen Jingyi, Cui Lei, Lu Songhui. 2019. Response of size-fractionated phytoplankton to environmental factors near the Changjiang Estuary. Acta Oceanologica Sinica, 38(1): 151–159, doi: 10.1007/s13131-018-1259-4

1 Introduction

Phytoplankton accounts for nearly half of the total global primary production (Falkowski et al., 1998). As the basis of the food web, phytoplankton serves as a bridge connecting inorganic compounds with organic matter that is available to higher trophic levels (Lohrenz et al., 1997; Yin et al., 2004). Thus, phytoplankton community dynamics remain a significant topic in the study of marine ecosystems (Cloern and Dufford, 2005; Butrón et al., 2009; Fu et al., 2016).

The size structure of phytoplankton assemblages controls the trophic organization of planktonic communities and their ability to export biogenic materials to the ocean's interior (Marañón, 2015). In addition, phytoplankton size structure responds to environmental variations (Malone, 1980; Platt and Silvert, 1981; Tamigneaux et al., 1999; Huete-Ortega et al., 2011). For example, phytoplankton communities are predicted to shift to smaller primary producers being dominant in response to warming (Morán et al., 2010; Polovina and Woodworth, 2012). In contrast, eutrophication may favor larger-sized cells because of their higher photosynthetic efficiency and higher growth rate (Tamigneaux et al., 1999; Cermeño et al., 2006; Fu et al., 2009). Thus, size-based partitioning of phytoplankton is a useful tool for monitoring key phytoplankton traits and provides a better understanding of phytoplankton dynamics (Fu et al., 2009).

Abiotic environmental factors, such as temperature, light, nutrient supply in the water and hydrodynamic conditions, have been considered important factors affecting the distribution of phytoplankton size structure in various marine ecosystems (Riegman et al., 1993; Agawin et al., 2000; Cermeño et al., 2005; Marañón et al., 2007). Furthermore, zooplankton grazing is important for regulating the size distribution of phytoplankton assemblages (Banse, 1992; Kiørboe, 1993).

The Changjiang Estuary is located in the East China Sea. The Changjiang River is the largest river in China in terms of volume. It plays an important role in the terrestrial inputs to the East China Sea, with a value of 9.32×10^{11} m^3/a (Chen et al., 2001; Chai et al., 2006; Zhou et al., 2012). Since the 1960s, high rates of population growth and economic development in the Changjiang Basin have resulted in a rapid increase in nutrient fluxes into the Changjiang Estuary. Consequently, eutrophication has become a more serious problem. Meanwhile, harmful algal blooms are a frequent occurrence in the adjacent East China Sea (Zhou et al., 2008, 2012; Wang et al., 2014). In addition, the impoundment of the Three Gorges Dam has resulted in notable hydrological variations, i.e., a decrease in river runoff and a lower current velocity in the Changjiang River, which may affect the phytoplankton community structure in the Changjiang Estuary and the adjacent sea (Jiao et al., 2007; Jia et al., 2014; Lian et al., 2014; Mei et al., 2015). Therefore, the marine ecological status of the Changjiang Estuary and the adjacent waters has garnered increased attention.

Many studies on phytoplankton size structure, including their

---

Foundation item: The National Basic Research Program (973 Program) of China under contract No. 2010CB428702; the Science and Technology Planning Project of Guangdong Province of China under contract No. 2016A030303012; the Strategic Priority Research Program of the Chinese Academy of Sciences under contract No. XDA11020304.

*Corresponding author, E-mail: lusonghui1963@163.com

spatial and temporal variations, have been carried out in the East China Sea (e.g., Li and Luan, 1998; Huang et al., 2006; Deng et al., 2008). However, near the Changjiang Estuary, dominant species were believed to be one of the main factors affecting the size fraction of phytoplankton biomass (Song et al., 2008; Zhou et al., 2012), and few studies are available that report on the response of phytoplankton size structure to environmental factors especially biotic factors. This study includes an investigation of the size-fractionated phytoplankton biomass in terms of chlorophyll *a* (Chl *a*) content and is aimed at (1) determining the variation in the size composition of phytoplankton to the total phytoplankton biomass during the spring and autumn of 2010 and (2) exploring the variation in phytoplankton size structure in relation to both abiotic (temperature and nutrients) and biotic (zooplankton) factors.

2 Materials and methods

2.1 *Sampling*

Field cruises were conducted in April 2010, May 2010 and October 2010 in the Changjiang Estuary and its adjacent sea. As illustrated in Fig. 1, the sampling sites were located at approximately 27.5°–32.5°N, 120°–124.2°E. A total of eight transects were conducted. Due to marine conditions and unfavorable weather conditions, the sampling stations and transects were not fixed. Detailed information about the cruises, sampling stations and transects are listed in Table 1.

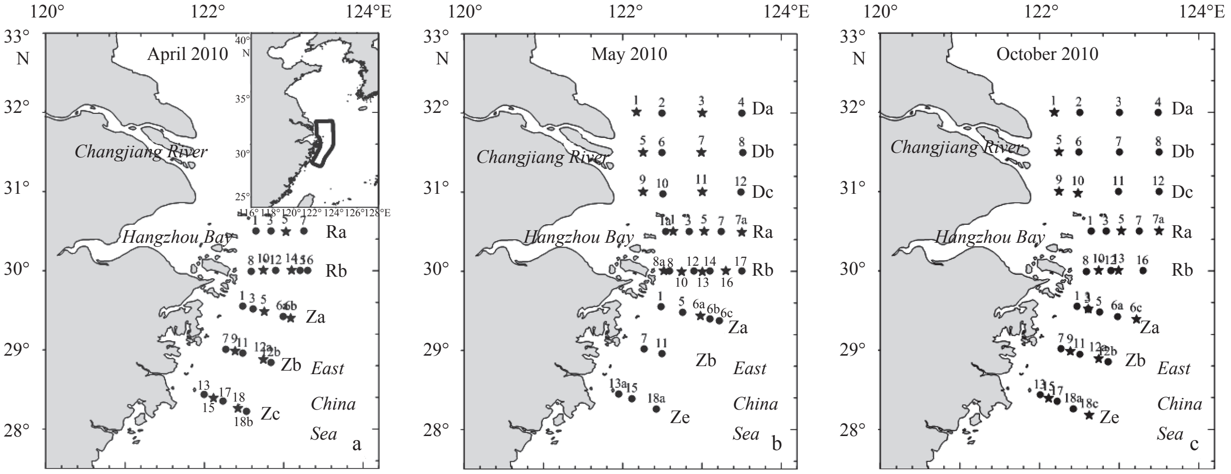

Fig. 1. Sampling stations in the Changjiang Estuary and adjacent coastal waters in the East China Sea. a. April 2010, b. May 2010, and c. October 2010. The circle dots indicate the stations where size-fractionated Chl *a* and environmental factors were measured during each cruise, while the stars indicate the stations where only environmental factors were measured during each cruise.

Table 1. Cruise information and the number of stations where size-fractionated Chl *a* was measured

Date of the cruise	Number of stations of size-fractionated Chl *a* measurement	Transects
Apr. 8–26	16	Ra, Rb, Za, Zb, Zc
May 7–26	22	Ra, Rb, Za, Zb, Zc, Da, Db, Dc
Oct. 7–13	24	Ra, Rb, Za, Zb, Zc, Da, Db, Dc

A CTD (Seabird 19 plus, Sea-Bird Electronics, USA) was used to measure seawater salinity and temperature. Surface samples for Chl *a*, nutrient, and phytoplankton were collected using 30 L Niskin bottles. The data on temperature, salinity, nutrients and zooplankton community are from a project supported by the National Basic Research Program of China.

2.2 *Size-fractionated Chl a*

The phytoplankton biomass was size-fractionated into meso- (>200 μm), micro- (20–200 μm), nano- (2–20 μm) and pico-phytoplankton (<2 μm). First, water samples were filtered through 200 μm and then 20 μm Nitex filters by gravity. The filtrates were serially filtered through 2 μm millipore polycarbonate nuclepore filters and 0.7 μm Whatman GF/F filters. The chlorophyll retained on the 200 μm filters was mesophytoplankton, and the chlorophyll remaining on the 20, 2.0 and 0.7 μm filters constituted the micro-, nano- and pico-phytoplankton fractions, respectively. For the total Chl *a* concentration, 200–1 000 mL of seawater was filtered through a 0.7 μm GF/F filter. Filtrates were immediately frozen in liquid nitrogen until the laboratory analysis. Pigments were extracted (in the cold and dark) for 16–24 h in 10 mL of 90% acetone. Chl *a* was measured fluorometrically by a Turner designs fluorometer (BWT2X7200) before and after acidification with 10% HCl (Parsons et al., 1984). The value of the meso-sized phytoplankton was considerably lower than the other size classes; therefore, the size classes of 20–200 μm and greater than 200 μm were combined into the micro-sized class (>20 μm) for data analysis.

2.3 *Nutrients analyses*

Seawater samples for the analyses of nutrients were filtered through precombusted GF/F filters. Filtrates were then analyzed onboard immediately for nitrate (N-NO_3^-), nitrite (N-NO_2^-), ammonium (N-NH_4^+), inorganic phosphorus (P-PO_4^{3-}) and dissolved silicon (Si-SiO_3^{2-}) using manual colorimetric methods according to the marine investigation criterion of China (State Oceanic Administration, 2008).

2.4 *Trophic conditions*

To characterize the trophic conditions of coastal marine waters, a parameter called the trophic state index (TRIX), put forward by Vollenweider et al. (1998) and modified by Giovanardi and Vollenweider (2004), was adopted. The TRIX is a linear combination of four variables related to eutrophication: Chl *a*, oxygen as absolute percent deviation from saturation conditions, nitrogen and phosphorus. Details for the TRIX (i_{tr}) are as follows:

$$i_{\mathrm{tr}}=\frac{[\lg\left(c_{\mathrm{ca}}\times c_{\mathrm{do}}\times c_{\mathrm{din}}\times c_{\mathrm{po_4}}\right)+1.5]}{1.2},$$

where c_{ca}, c_{do}, c_{din} and $c_{\mathrm{po_4}}$ represent Chl *a*, DO%, DIN and PO_4 concentrations, respectively.

Values more than six TRIX units mean that the coastal waters are hypereutrophic, whereas values lower than four TRIX units are usually associated with oligotrophic coastal waters. In the open sea, values are generally less than three TRIX units.

2.5 *Microscopic analysis of phytoplankton composition*

One thousand milliliters of seawater samples were placed in Pyrex bottles, and fixed with Lugol's solution (4% final concentration). For microscopic observation, a volume of 10 mL of each sample was settled in a settling chamber for at least 24 h and examined under a Nikon E200 microscope to identify and enumerate phytoplankton taxa following the Utermöhl method (Utermöhl, 1958).

2.6 *Zooplankton analysis*

Samples for zooplankton analysis were collected with a plankton net (mesh size 505 μm, diameter 50 cm). The net was hauled vertically from the bottom to the surface. The samples were immediately fixed with 5% formalin for further identification of species under the microscope.

2.7 *Data analysis*

Seasonal differences among the various variables were analyzed by one-way ANOVA tests. Prior to the test, the homogeneity of a variance test was performed to check the validation of the ANOVA tests. If this test failed, data were log-transformed. The chlorophyll content of each phytoplankton size class was related to various variables reported on the basis of the Pearson correlation analysis.

3 Results

3.1 *Overview*

The cruise time series during the spring of 2010 covered two different phases. No dinoflagellate blooms were observed during April 2010. The average abundance of phytoplankton was 1.99×10^5 cell/L. The phytoplankton community was dominated by diatoms, consisting primarily of chain-forming species, such as *Pseudo-nitzschia* spp. and *Skeletonema* spp. In addition, dinoflagellates, such as *Prorocentrum donghaiense*, were occasionally abundant in the southern part of the study area. During May 2010, *P. donghaiense* blooms, peaking at 3.7×10^6 cell/L at Station Zc13, were observed in almost the entire study area, accounting for more than three quarters of the total phytoplankton abundance.

In the autumn of 2010, the average abundance of phytoplankton was 2.37×10^4 cell/L, ranging from 1.35×10^2 to 1.17×10^5 cell/L. Although dinoflagellates dominated the phytoplankton community, their abundance was one or more orders of magnitude lower than that in May 2010. *P. donghaiense* were numerically predominant, occupying 26.9% of the total phytoplankton abundance.

3.2 *Hydrological factors*

In April 2010, the water temperature increased gradually from nearshore to offshore (Fig. 2a), ranging from 11.1 to 16.6°C. The salinity followed a similar trend as the temperature (Fig. 2d), ranging from 24.0 and 33.2. In May 2010, the water temperature increased to above 15°C. High water temperature values were observed in the eastern locations of the Changjiang Estuary (Fig. 2b). In October 2010, the water temperatures were notably higher than those recorded during the other two cruises ($P<0.01$), averaging 23.3°C. The highest temperature was observed in the southeastern part of the study area. Lower temperature waters were distributed near the mouth of the Hangzhou Bay (Fig. 2c). The salinity was influenced by the diluted water of the Changjiang River; values from the near-shore waters were consistently lower than those from offshore waters (Figs 2d–f). In May 2010 and October 2010, the salinity at Station Db5, close to the mouth of the Changjiang Estuary, was only 5.7 and 10.0, respectively.

3.3 *Nutrients*

The distribution patterns of the nutrient concentrations during the three cruises are illustrated in Fig. 3. Since Si-SiO_3^{2-} and P-PO_4^{3-} concentrations showed a similar spatial pattern to that of N-NO_3^-, while N-NO_2^- and N-NH_4^+ in general constituted a smaller proportion (less than 10% at most stations) of the dissolved inorganic nitrogen (DIN) and displayed no perceptible spatial patterns, only the spatial distribution of the N-NO_3^- concentrations was described in detail for the three cruises. With respect to the other inorganic nutrients, only the range, the mean and standard deviation values are presented in Table 2.

As illustrated in Fig. 3, the general spatial patterns of N-NO_3^- concentrations decreased from nearshore to offshore. In May 2010, the higher concentrations of N-NO_3^- were in the northwestern part of the study area (Fig. 3b). In October 2010, high levels of N-NO_3^- were observed in the middle part of the study area (Fig. 3c). The temporal variability revealed that the N-NO_3^- and Si-SiO_3^{2-} concentrations in April 2010 were higher than those in October 2010 ($P<0.05$) (Table 2). For the P-PO_4^{3-} concentrations, no significant differences were found between April 2010 and October 2010 ($P>0.05$). When comparing the nutrient concentrations during the two phases in the spring of 2010, the results showed that the *P. donghaiense* bloom significantly decreased the P-PO_4^{3-} concentrations ($P<0.01$), whereas the N-NO_3^- and Si-SiO_3^{2-} concentrations showed no significant differences between the two phases ($P>0.05$).

The TRIX varied between 4.02 and 6.44 in the spring of 2010, with 20% of the values being higher than 6 (threshold values of hypereutrophic). In the autumn of 2010, the TRIX ranged from 2.96 to 5.55. The seasonal variability revealed that the TRIX in the spring were higher than those in autumn ($P<0.01$).

3.4 *Total Chl a and size-fractionated Chl a concentrations*

In April 2010, the total Chl *a* values varied from 0.25 to 6.15 μg/L, with a mean of 2.16 μg/L. The lowest values of phytoplankton Chl *a* were found at the mouth of Hangzhou Bay and in the nearshore waters of the survey area. Higher Chl *a* concentrations were found in the southeastern part of the study area (Fig. 4a). Micro-Chl *a* content ranged between 0.02 and 1.25 μg/L. High microphytoplankton biomass was found in the central waters of the study area (Fig. 4b). The nano- and pico-sized Chl *a* exhibited similar trends (Figs 4c and d).

In May 2010, the total Chl *a* concentration varied between 0.07 and 18.7 μg/L. The breakout of the *P. donghaiense* bloom

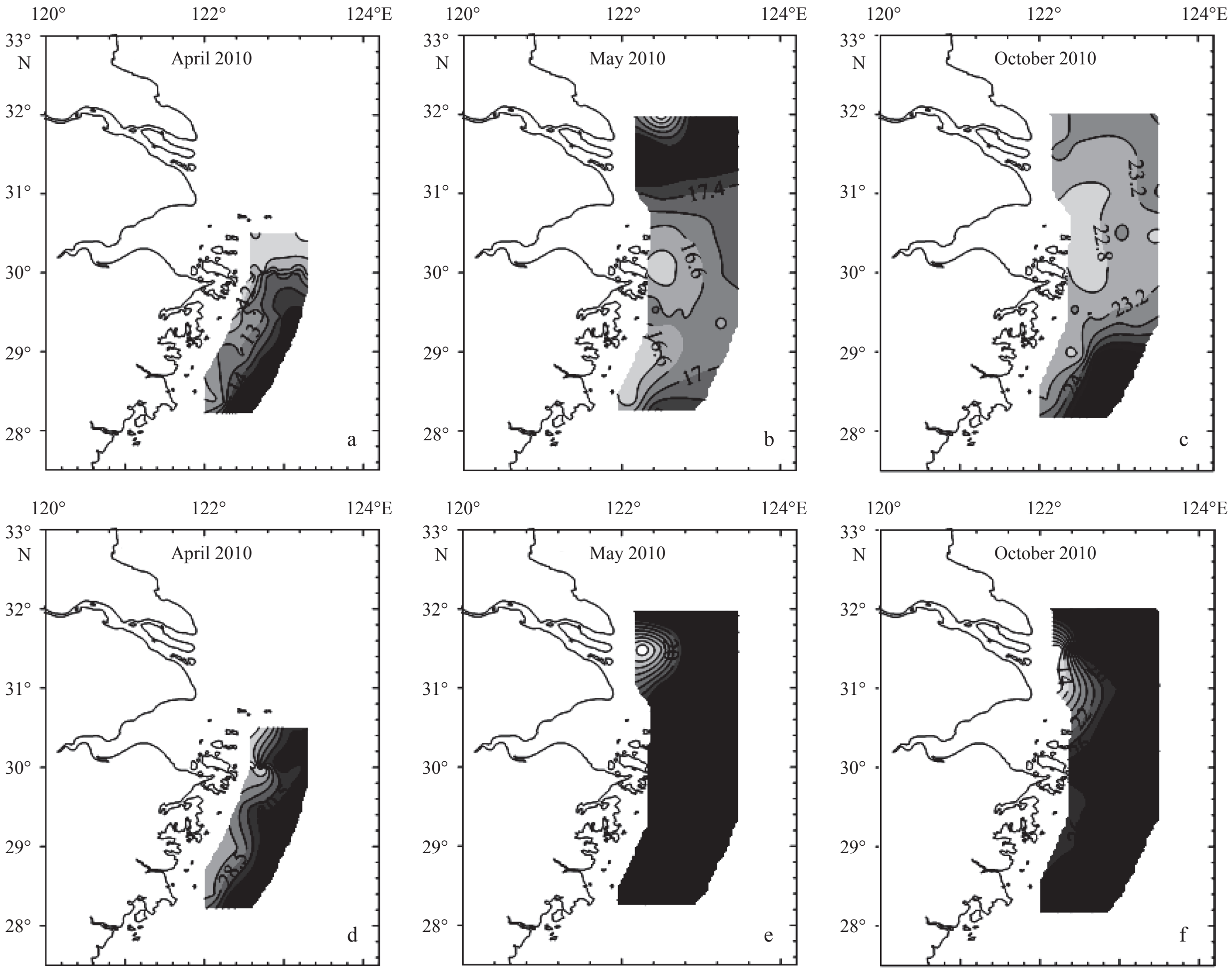

Fig. 2. Spatial distribution patterns of temperature (°C) (a, b, c) and salinity (d, e, f) at the surface layer.

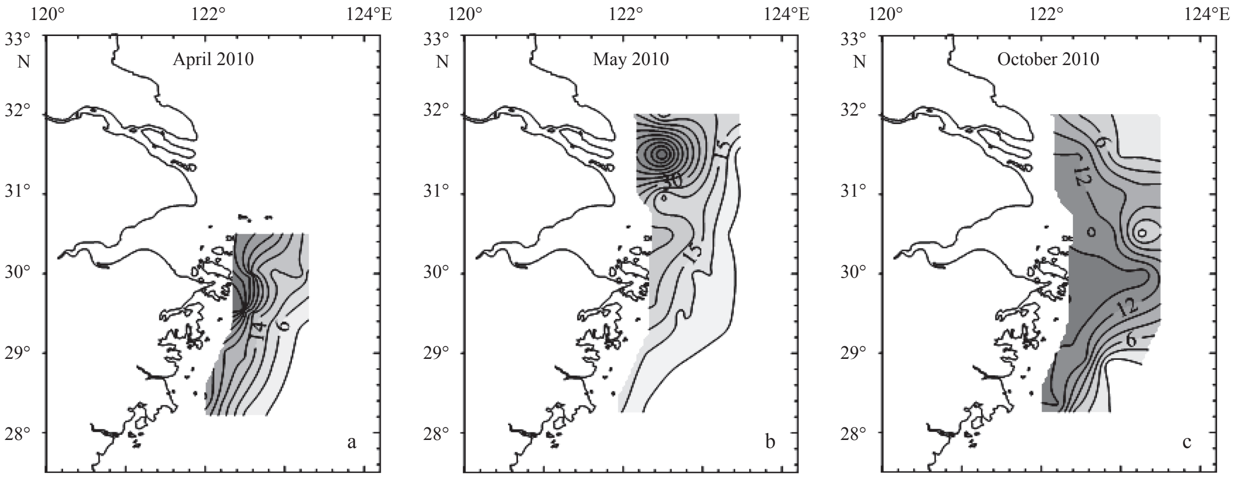

Fig. 3. Spatial distribution patterns of nitrate concentrations (μmol/L) at the surface layer.

considerably elevated the Chl *a* concentration, with a mean value up to 4.29 μg/L. The region of high Chl *a* shifted towards the nearshore waters of the southern part of the study area (Fig. 4e). A high concentration of micro-Chl *a* was found near the mouth of the Hangzhou Bay (Fig. 4f). Nano-Chl *a* concentrations, in the range of 0.17 to 15.7 μg/L, exhibited a similar trend as the total Chl *a* concentration, with the Chl *a* concentration distribution gradually decreasing seaward (Fig. 4g).

In the autumn of 2010, the Chl *a* concentrations were markedly lower than the values in the spring and were highly variable throughout the study area. The total Chl *a* concentration varied from 0.01 to 0.65 μg/L, with a mean value of 0.30 μg/L. The high Chl *a* concentrations were usually located in the southwestern part of the study area (Fig. 4i). An additional patch of high Chl *a*

Table 2. Nutrient concentrations measured during the three cruises at the surface layer

		N-NO_3^- /μmol·L^{-1}	N-NO_2^- /μmol·L^{-1}	N-NH_4^+ /μmol·L^{-1}	Si-SiO_3^{2-} /μmol·L^{-1}	P-PO_4^{3-} /μmol·L^{-1}
April	range	4.18–45.8	0.22–0.63	0.2–2.25	2.00–33.22	0.05–1.04
	mean±SE	18.76±10.99	0.45±0.13	0.80±0.52	18.07±10.06	0.47±0.32
May	range	0.2–71.92	0.03–1.22	0.38–1.59	9.49–76.44	0.04–1.32
	mean±SE	13.89±14.14	0.47±0.24	1.04±0.33	20.98±13.54	0.19±0.28
October	range	0–15.72	0.16–1.57	0.36–2.06	2.26–17.8	0.02–1.16
	mean±SE	9.58±5.31	0.80±0.39	0.99±0.47	10.79±5.17	0.45±0.35

Note: SE is abbreviated from standard error.

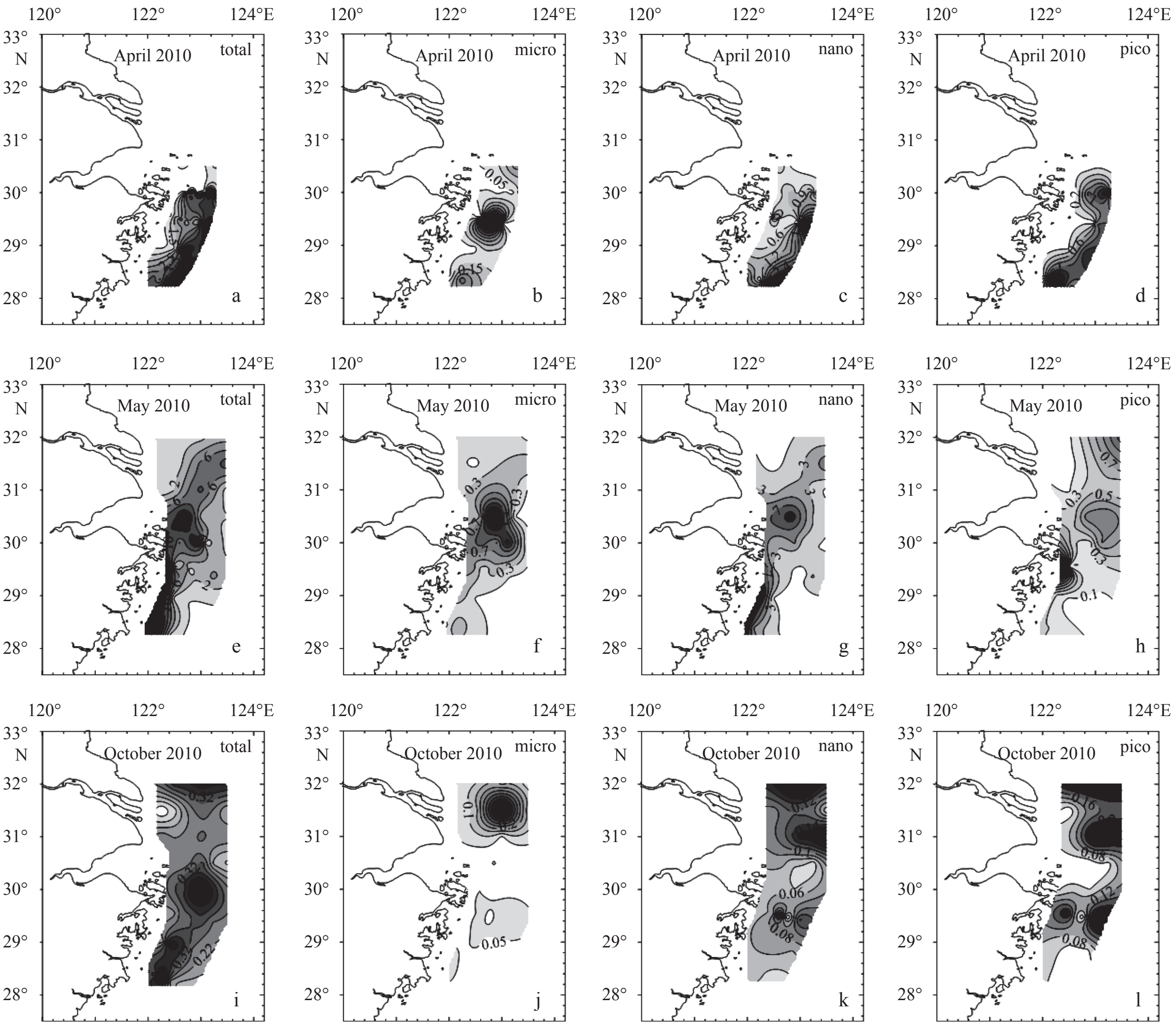

Fig. 4. Spatial distribution of total Chl *a* and the micro-, nano- and pico-sized fractionated Chl *a* concentrations (μg/L) at the surface layer.

concentration was observed near 30°N, 123°E. The lowest Chl *a* concentrations were observed near the Changjiang Estuary (Fig. 4i). High concentrations of microphytoplankton Chl *a* were east of the Changjiang Estuary (Fig. 4j). In the remaining study area, the micro-Chl *a* concentration generally varied between 0.01 and 0.12 μg/L, and the nano-Chl *a* concentrations varied between 0.02 and 0.25 μg/L.

3.5 *Contributions of size-fractionated Chl a*

As illustrated in Fig. 5, the phytoplankton community in April 2010 was dominated by nanophytoplankton, comprising over 60% of the phytoplankton biomass at most of the sampling stations (Fig. 5).

In May 2010, nanophytoplankton was the absolutely predominant fraction; more than 90% of the Chl *a* biomass was composed of the nanoplankton fraction (33.4%–97.7%) (Fig. 5). The percentages of microphytoplankton and picophytoplankton were 0%–53.7% (12.6%) and 0%–46.1% (13.8%), respectively.

In the autumn of 2010, nano- (37.0%) and picophytoplankton (34.4%) collectively dominated the phytoplankton community. It can be seen that nanophytoplankton decreased its predominance and constituted (2.5%–58.0%) considerably lower fractions than those of the two spring cruises ($P<0.01$) (Fig. 5). Excluding a few of the stations, the percentage of the nano-sized fraction was

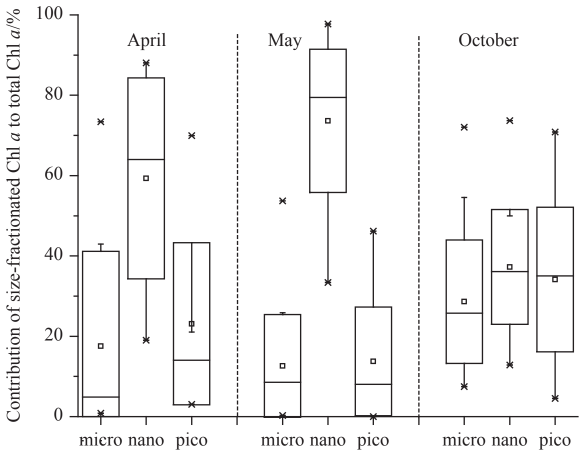

Fig. 5. Temporal distribution of percentages of the micro-, nano- and pico-sized fractionated Chl *a* concentrations to the total Chl *a* concentration.

generally less than 50.0% (Fig. 5). Conversely, the pico-sized and micro-sized fraction tended to increase in contribution, accounting for 4.5%–70.8% (34.4%) and 7.5%–66.5% (26.1%) of the phytoplankton biomass, respectively.

3.6 *Zooplankton abundance and dominant species*

The zooplankton abundance ranged from 10.8 to 2.4×10^3 ind./L. The maximum zooplankton abundance was observed during April 2010 at Station Za1, while the minimum zooplankton abundance occurred during October 2010 at Station Db5. The abundance of zooplankton during October 2010 was approximately one-sixth of the quantity of the other two cruises. The dominant population of zooplankton exhibited an obvious seasonal transition. During the two spring cruises, the total abundance of zooplankton ranged from 37.6 to 2.4×10^3 ind./L and 16.3 to 1.9×10^3 ind./L. The dominant taxon was the copepod, *Calanus sinicus*, averaging 76.6% (range of 33%– 97%) and 67.4% (range of 6.3%–97.9%) of the total abundance for the two cruises (Fig. 6). The zooplankton community shifted from the ubiquitous *C. sinicus* towards *Sagitta enflata* in autumn (Fig. 6). However, the contribution of *S. enflata* to the total abundance averaged 23.8% (range of 0%–61.7%), which was much lower than that of *C. sinicus* in the other two spring cruises. Other major taxa included *Euchaeta larvae* (18.0%), *Eucalanus subcrassus* (8.8%), *C. sinicus* (5.8%) and *Sagitta bedoti* (5.0%) (Fig. 6).

3.7 *Relationship between Chl a concentration and environmental factors*

The results of the Pearson relation analyses of the relationships between the Chl *a* concentration of the size-fractionated Chl *a* and various environment properties are listed in Table 3. The Chl *a* concentrations of all of the three fractions showed significant, negative correlations with the P-PO$_4^{3-}$ concentrations ($P<0.01$ or less than 0.05). Furthermore, nano-Chl *a* concentrations was positively correlated with the TRIX, copepod abundance as well as zooplankton abundance ($P<0.01$) (Table 3).

For the relative contribution of different Chl *a* variables, the micro-sized fraction Chl *a* displayed a negative correlation with Si-SiO$_3^{2-}$, TRIX, copepod abundance and zooplankton abundance ($P<0.01$ or less than 0.05) (Table 3). The nano-sized fraction was correlated positively with DIN, Si-SiO$_3^{2-}$, TRIX, copepod abundance and zooplankton abundance (Table 3) ($P<0.01$ or less than 0.05); it was negatively correlated with the temperature ($P<0.01$). A significant negative correlation between the pico-sized fraction and some nutrients (DIN, Si-SiO$_3^{2-}$) concentration, TRIX as well as copepod abundance ($P<0.01$ or $P<0.05$) was observed. In addition, the relative contribution of picophytoplankton was positively correlated with the temperature ($P<0.01$).

4 Discussion

4.1 *Seasonal shift in the phytoplankton size structure*

It appeared that there was a seasonal shift in the ratio of the different size classes of phytoplankton to the total Chl *a* concen-

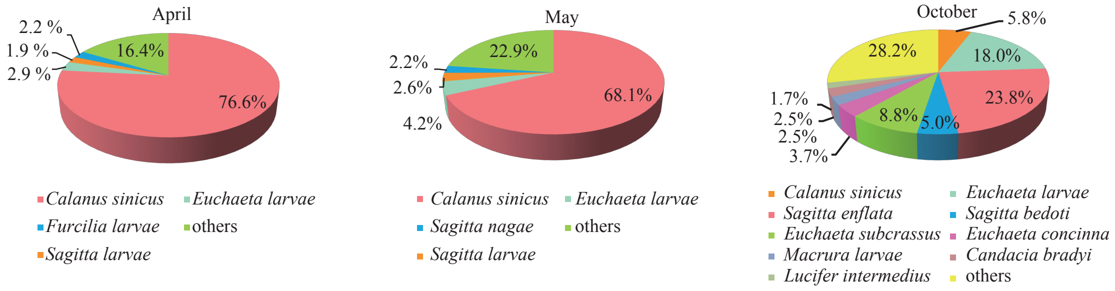

Fig. 6. Zooplankton community structure in the Changjiang Estuary.

Table 3. Pearson correlation coefficients and significance between size-fractionated Chl *a* concentrations and their contributions to the total Chl *a* versus environmental variables

	T	DIN	P-PO$_4^{3-}$	Si-SiO$_3^{2-}$	TRIX	Copepod abundance	Zooplankton abundance
Micro-Chl *a*/μg·L^{-1}	$-0.204^{\text{n.s.}}$	$0.001^{\text{n.s.}}$	-0.295^{*}	$0.027^{\text{n.s.}}$	$0.080^{\text{n.s.}}$	0.024	−0.020
Nano-Chl*a*/μg·L^{-1}	$-0.223^{\text{n.s.}}$	$0.001^{\text{n.s.}}$	-0.309^{*}	$0.195^{\text{n.s.}}$	0.439^{**}	0.450^{**}	0.352^{**}
Pico-Chl *a*/μg·L^{-1}	$-0.236^{\text{n.s.}}$	$-0.064^{\text{n.s.}}$	-0.361^{**}	$-0.085^{\text{n.s.}}$	$0.130^{\text{n.s.}}$	0.250^{*}	0.221
Micro-Chl *a*/%	$0.153^{\text{n.s.}}$	$-0.051^{\text{n.s.}}$	$0.062^{\text{n.s.}}$	-0.252^{*}	-0.279^{*}	-0.338^{**}	-0.290^{*}
Nano-Chl *a*/%	-0.425^{**}	0.272^{*}	$0.028^{\text{n.s.}}$	0.551^{**}	0.445^{**}	0.363^{**}	0.287^{*}
Pico-Chl *a*/%	0.331^{**}	-0.257^{*}	$-0.091^{\text{n.s.}}$	-0.450^{**}	-0.362^{**}	-0.296^{*}	−0.229

Note: n.s. represents $P>0.05$; * $P<0.05$; ** $P<0.01$.

tration in the area near the Changjiang Estuary. Nanophytoplankton were the dominant contributor in the spring (Fig. 5), accounting for more than 60.0% of the phytoplankton biomass in most of the sampling stations. In October, the phytoplankton community was primarily composed of picophytoplankton and nanophytoplankton. It is common for seasonal variations to occur in phytoplankton community structures in estuaries and the adjacent areas. Qiu et al. (2010) observed this type of shift in the Zhujiang Estuary and the adjacent near shore oceanic water, which was similar to the results of Buchanan et al. (2005) for the Chesapeake Bay.

4.2 *Environmental regulation of phytoplankton size structure*

The size-fractionated biomass of the phytoplankton changed according to temperature; small cells increased with increasing temperature (Mousing et al., 2014). This result might explain why picophytoplankton increases in importance in the autumn when temperatures were considerably higher than those in the spring. The Pearson correlation analysis indicated a significantly positive correlation between the percent contribution of pico-Chl *a* and temperature ($P<0.01$) when data from all seasons were pooled. Furthermore, the relative abundance of nanophytoplankton decreased with increasing temperature ($P<0.01$). This result is consistent with the results from a previous study in Arctic waters, which showed a significant relationship between size classes of phytoplankton biomass (decrease in nanoplankton and increase in picoplankton) and an increase in water temperature (Li et al., 2009; Hilligsøe et al., 2011). This correlation indicates that water temperature might play a fundamental role in controlling the size distribution of phytoplankton communities. However, it is still controversial whether temperature has a direct effect on phytoplankton size structure, since temperature and nutrient supply are strongly negatively correlated in the ocean (Kamykowski and Zentara, 1986; Agawin et al., 2000).

It is widely accepted that the contribution of picophytoplankton biomass to total phytoplankton biomass increased from eutrophic waters to oligotrophic waters (Agawin et al., 2000; Marañón et al., 2001; Gaulke et al., 2010; Kulk et al., 2012). In the present study, when the Chl *a* values from all cruises were pooled, the percent contribution of picophytoplankton Chl *a* to total Chl *a* was negatively correlated with DIN, Si-SiO_3^{2-} and TRIX (Table 3), which is relatively consistent with the general patterns observed in previous studies.

The microphytoplantkon species have higher nutrient uptake rates, allowing them to have a competitive advantage for nutrients relative to the smaller cells in eutrophic systems (Riegman et al., 1993; Gaulke et al., 2010). Thus, the lower nutrient concentrations and lower TRIX in the autumn of 2010 relative to the spring of 2010 led to the expectation that microphytoplankton would contribute less to the total phytoplankton biomass. In contrast, the relative contribution of microphytoplankton biomass to the total phytoplankton biomass in the autumn of 2010 increased significantly compared to that in the spring of 2010. The result of the Pearson correlation analysis indicated that a significantly negative correlation among Si-SiO_3^{2-} concentrations, TRIX and the contribution of microphytoplankton to total Chl *a*. This result is consistent with those obtained in previous studies in the Zhujiang Estuary (Li et al., 2013), and the Mdloti and Mhlanga estuaries (Thomas et al., 2005). The reason why the microphytoplankton increase in its importance under lower trophic condition may be explained by the grazing pressure of zooplankton. As previously mentioned, zooplankton grazing plays an important role in controlling the phytoplankton size structure. Mesozooplankton dominated by copepods are more likely to ingest large phytoplankton (Uye, 1986; Bautista and Harris, 1992; Nejstgaard et al., 1995; Hansen et al., 2000; Tan et al., 2004). In the present study, the abundance of copepods displayed a negative correlation with the relative abundance of microphytoplankton. In the spring of 2010, copepods were the most abundant mesozooplankton, while their abundance as well as their contribution to total abundance significantly decreased in the autumn of 2010. Thus, during the autumn of 2010, the grazing pressure of mesozooplankton on microphytoplankton was relatively low. The low grazing pressure is the most likely reason for the increasing importance of microphytoplankton under lower nutrient concentrations conditions during the autumn of 2010. For nanophytoplankton, a strong positive correlation was observed between the percentage of nanophytoplankton and TRIX (Table 3), suggesting that changes in the nanophytoplankton community structure could reflect nanophytoplankton responses to the trophic conditions.

4.3 *Relationship between phytoplankton size structure and anthropogenic perturbations*

Because of the rapid development of the economy and the agriculture, as well as an increase in the population, the continental nutrient fluxes into the East China Sea have notably increased over the past few decades (Zhang et al., 1999; Zhou et al., 2001, 2003; Li et al., 2014). However, the nitrogen and phosphorus due to anthropogenic loading of nutrients usually increased disproportionately (e.g., Chai et al., 2006; Zhou et al., 2008), which resulted in a shift in the nutrient regime in the study area. A high N:P ratio and phosphate limitation have been characteristics of the Changjiang Estuary and adjacent coastal areas in the spring (Zhou et al., 2008). According to Justić et al. (1995), phosphorus limitation occurs if the ratio of silicon to phosphorus concentrations is greater than 22 and the ratio of nitrogen to phosphorus concentrations is greater than 22 (Justić et al., 1995). During our study, in the spring, the ratio of nitrogen to phosphorus concentrations generally exceeded 16:1 (22.4% even more than 100:1), and more than 80% of stations exhibited potential phosphorus limitation.

A high ratio of nitrogen to phosphorus and phosphorus limitation are believed to be responsible for the shift of HAB causative species from diatoms to dinoflagellates (Zhou et al., 2008). To date, large-scale dinoflagellate blooms of *P. donghaiense* in the study area in the late spring and early summer have been recurrent for no less than 10 a (Lu et al., 2005, 2014). It has been reported that flagellates are highly efficienct in the absorption of phosphorus (Egge, 1998), which might explain why the P-PO_4^{3-} concentrations significantly decrease during the *P. donghaiense* blooms in our study.

Prorocentrum donghaiense (asymmetric and elongated, 18.6–21.6 μm long, and 9.6–13.0 μm wide) is a type of nano-sized phytoplankton (Lu et al., 2005). The bloom during the study period significantly increased the Chl *a* concentrations of nanophytoplankton, as well as their contribution to the total phytoplankton biomass. Nano-sized Chl *a* concentrations increased from 1.08 to 4.53 μg/L, and contributions to the total Chl *a* ranged from 59.3% to 76.2%. Therefore, variations in phytoplankton size structure might be an indicator of the ecological effects of anthropogenic perturbations, and high-frequency sampling is required to capture the response of phytoplankton size structure to environmental changes.

5 Conclusions

In summary, the variations of size-fractionated Chl *a* during the spring and autumn of 2010 and the response of different size classes to environmental disturbances are presented for the Changjiang Estuary.

The highlights of this study include the following:

(1) The dominance of nanophytoplankton and/or picophytoplankton over microphytoplankton reflecs the eutrophic conditions in the Changjiang Estuary.

(2) A different pattern of the phytoplankton size structure with nanophytoplankton dominance occurs in the spring and nanophytoplankton and picophytoplankton co-dominance occurs in the autumn.

(3) Water temperature and trophic conditions are the main factors influencing the importance of nano- and pico-sized Chl *a*.

(4) The potential link between the contribution of microphytoplankton increases in the autumn as well as the grazing pressure exerted by mesozooplankton (copepods).

Acknowledgements

We acknowledge the captain and crew of R/V *Zhe Hai Huan Jian* for their help in sampling and sample processing. We thank the Second Institute of Oceanography, Ministry of Natural Resources of China, the East China Sea Fisheries Research Institute and the Chinese Academy of Fisheries Sciences for providing temperature, salinity, nutrient and zooplankton data.

References

Agawin N R S, Duarte C M, Agustí S. 2000. Nutrient and temperature control of the contribution of picoplankton to phytoplankton biomass and production. Limnology and Oceanography, 45: 591–600, doi: 10.4319/lo.2000.45.3.0591

Banse K. 1992. Grazing, temporal changes of phytoplankton concentrations, and the microbial loop in the open sea. In: Falkowski P G, Woodhead A D, Vivirito K, eds. Primary Productivity and Biogeochemical Cycles in the Sea. Boston, MA: Springer, 409–440

Bautista B, Harris R P. 1992. Copepod gut contents, ingestion rates and grazing impact on phytoplankton in relation to size structure of zooplankton and phytoplankton during a spring bloom. Marine Ecology Progress Series, 82: 41–50, doi: 10.3354/meps082041

Buchanan C, Lacouture R V, Marshall H G, et al. 2005. Phytoplankton reference communities for Chesapeake Bay and its tidal tributaries. Estuaries, 28: 138–159, doi: 10.1007/BF02732760

Butrón A, Iriarte A, Madariage I. 2009. Size-fractionated phytoplankton biomass, primary production and respiration in the Nervión-Ibaizabal Estuary: a comparison with other nearshore coastal and estuarine ecosystems from the Bay of Biscay. Continental Shelf Research, 29: 1088–1102, doi: 10.1016/j.csr.2008.11.013

Cermeño P, Marañón E, Rodríguez J, et al. 2005. Large-sized phytoplankton sustain higher carbon-specific photosynthesis than smaller cells in a coastal eutrophic ecosystem. Marine Ecology Progress Series, 297: 51–60, doi: 10.3354/meps297051

Cermeño P, Maraón E, Pérez V, et al. 2006. Phytoplankton size structure and primary production in a highly dynamic coastal ecosystem (Ría de Vigo, NW-Spain): Seasonal and short-time scale variability. Estuarine, Coastal and Shelf Science, 67: 251–266, doi: 10.1016/j.ecss.2005.11.027

Chai Chao, Yu Zhiming, Song Xiuxian, et al. 2006. The status and characteristics of eutrophication in the Yangtze River (Changjiang) Estuary and the adjacent East China Sea, China. Hydrobiologia, 563: 313–328, doi: 10.1007/s10750-006-0021-7

Chen Zhongyuan, Li Jiufa, Shen Huanting, et al. 2001. Yangtze River of China: historical analysis of discharge variability and sediment flux. Geomorphology, 41: 77–91, doi: 10.1016/S0169-555X(01)00106-4

Cloern J E, Dufford R. 2005. Phytoplankton community ecology: principles applied in San Francisco Bay. Marine Ecology Progress Series, 285: 11–28, doi: 10.3354/meps285011

Deng Chunmei, Yu Zhigang, Yao Peng, et al. 2008. Size-fractionated phytoplankton in the East China and southern Yellow Seas and its environmental factors in autumn 2000. Periodical of Ocean University of China (in Chinese), 38: 791–798

Egge J K. 1998. Are diatoms poor competitors at low phosphate concentrations? Journal of Marine Systems, 16: 191–198, doi: 10.1016/S0924-7963(97)00113-9

Falkowski P G, Barber R T, Smetacek V. 1998. Biogeochemical controls and feedbacks on ocean primary production. Science, 281: 200–206, doi: 10.1126/science.281.5374.200

Fu Mingzhu, Wang Zongling, Li Yan, et al. 2009. Phytoplankton biomass size structure and its regulation in the southern Yellow Sea (China): seasonal variability. Continental Shelf Research, 29: 2178–2194, doi: 10.1016/j.csr.2009.08.010

Fu Tingting, Chen Baohong, Ji Weidong, et al. 2016. Size structure of phytoplankton community and its response to environmental factors in Xiamen Bay, China. Environmental Earth Sciences, 75(9): 734, doi: 10.1007/s12665-016-5552-2

Gaulke A K, Wetz M S, Paerl H W. 2010. Picophytoplankton: a major contributor to planktonic biomass and primary production in a eutrophic, river-dominated estuary. Estuarine, Coastal and Shelf Science, 90: 45–54, doi: 10.1016/j.ecss.2010.08.006

Giovanardi F, Vollenweider R A. 2004. Trophic conditions of marine coastal waters: experience in applying the trophic index TRIX to two areas of the Adriatic and Tyrrhenian Seas. Journal of Limnology, 63: 199–218, doi: 10.4081/jlimnol.2004.199

Hansen B W, Hygum B H, Brozek M, et al. 2000. Food web interactions in a *Calanus finmarchicus* dominated pelagic ecosystem-A mesocosm study. Journal of Plankton Research, 22: 569–588, doi: 10.1093/plankt/22.3.569

Hilligsøe K M, Richardson K, Bendtsen J, et al. 2011. Linking phytoplankton community size composition with temperature, plankton food web structure and sea-air CO_2, flux. Deep-Sea Research: Part I. Oceanographic Research Papers, 58: 826–838, doi: 10.1016/j.dsr.2011.06.004

Huang Bangqin, Liu Yuan, Chen Jixin, et al. 2006. Temporal and spatial distribution of size-fractionized phytoplankton biomass in East China Sea and Huanghai Sea. Acta Oceanologica Sinica (in Chinese), 28: 156–164

Huete-Ortega M, Calvo-Díaz A, Graña R, et al. 2011. Effect of environmental forcing on the biomass, production and growth rate of size-fractionated phytoplankton in the central Atlantic Ocean. Journal of Marine Systems, 88: 203–213, doi: 10.1016/j.jmarsys.2011.04.007

Jia Haibo, Shao Junbo, Hu Haoyan, et al. 2014. Changes and reason analysis of phytoplankton community structure in the Yangtze Estuary and adjacent sea before and after the impoundment of the Three Gorges Dam. Marine Science Bulletin, 33: 305–314

Jiao Nianzhi, Zhang Yao, Zeng Yonghui, et al. 2007. Ecological anomalies in the East China Sea: impacts of the Three Gorges Dam?. Water Research, 41: 1287–1293, doi: 10.1016/j.watres.2006.11.053

Justić D, Rabalais N N, Turner R E, et al. 1995. Changes in nutrient structure of river-dominated coastal waters: stoichiometric nutrient balance and its consequences. Estuarine, Coastal and Shelf Science, 40: 339–356, doi: 10.1016/S0272-7714(05)80014-9

Kamykowski D, Zentara S J. 1986. Predicting plant nutrient concentrations from temperature and sigma-*t*, in the upper kilometer of the world ocean. Deep-Sea Research: Part A. Oceanographic Research Papers, 33: 89–105, doi: 10.1016/0198-0149(86)90109-3

Kiørboe T. 1993. Turbulence, phytoplankton cell size, and the structure of pelagic food webs. Advances in Marine Biology, 29: 1–72, doi: 10.1016/S0065-2881(08)60129-7

Kulk G, de Vries P, van de Poll W H, et al. 2012. Temperature-dependent growth and photophysiology of prokaryotic and eukaryotic oceanic picophytoplankton. Marine Ecology Progress Series, 466: 43–55, doi: 10.3354/meps09898

Li Li, Lu Songhui, Jiang Tao, et al. 2013. Seasonal variation of size-fractionated phytoplankton in the Pearl River estuary. Chinese Science Bulletin, 58: 2303–2314, doi: 10.1007/s11434-013-5823-1

Li Chaolun, Luan Fenghe. 1998. A proliminary study on the distribution of size-fractionated chlorophyll-a in the euphotic zone of the East China Sea in spring. Marine Sciences (in Chinese), 22(4): 59–62

Li W K W, McLaughlin F A, Lovejoy C, et al. 2009. Smallest algae thrive as the Arctic Ocean freshens. Science, 326: 539, doi: 10.1126/science.1179798

Li Hongmei, Tang Hongjie, Shi Xiaoyong, et al. 2014. Increased nutrient loads from the Changjiang (Yangtze) River have led to increased harmful algal blooms. Harmful Algae, 39: 92–101, doi: 10.1016/j.hal.2014.07.002

Lian Jijian, Yao Ye, Ma Chao, et al. 2014. Reservoir operation rules for controlling algal blooms in a tributary to the impoundment of Three Gorges Dam. Water, 6: 3200–3223, doi: 10.3390/w6103200

Lohrenz S E, Fahnenstiel G L, Redalje D G, et al. 1997. Variations in primary production of Northern Gulf of Mexico continental shelf waters linked to nutrient inputs from the Mississippi River. Marine Ecology Progress Series, 155: 45–54, doi: 10.3354/meps155045

Lu Douding, Goebel J, Qi Yuzao, et al. 2005. Morphological and genetic study of *Prorocentrum donghaiense* Lu from the East China Sea, and comparison with some related Prorocentrum species. Harmful Algae, 4: 493–505, doi: 10.1016/j.hal.2004.08.015

Lu Douding, Qi Yuzao, Gu Haifeng, et al. 2014. Causative species of harmful algal blooms in Chinese coastal waters. Algological Studies, 145-146: 145–168

Malone T C. 1980. Algal size. In: Morris I, ed. The Physiological Ecology of Phytoplankton. Oxford: Blackwell Scientific, 433–463

Marañón E. 2015. Cell size as a key determinant of phytoplankton metabolism and community structure. Annual Review of Marine Science, 7: 241–264, doi: 10.1146/annurev-marine-010814-015955

Marañón E, Cermeño P, Rodríguez J, et al. 2007. Scaling of phytoplankton photosynthesis and cell size in the ocean. Limnology and Oceanography, 52: 2190–2198, doi: 10.4319/lo.2007.52.5.2190

Marañón E, Holligan P M, Barciela R, et al. 2001. Patterns of phytoplankton size structure and productivity in contrasting open-ocean environments. Marine Ecology Progress Series, 216: 43–56, doi: 10.3354/meps216043

Mei Xuefei, Dai Zhijun, Van Gelder P H A J M, et al. 2015. Linking Three Gorges Dam and downstream hydrological regimes along the Yangtze River, China. Earth and Space Science, 2: 94–106, doi: 10.1002/ess2.v2.4

Morán X A G, López-Urrutia Á, Calvo-Díaz A, et al. 2010. Increasing importance of small phytoplankton in a warmer ocean. Global Change Biology, 16: 1137–1144, doi: 10.1111/gcb.2010.16.issue-3

Mousing E A, Ellegaard M, Richardson K. 2014. Global patterns in phytoplankton community size structure-evidence for a direct temperature effect. Marine Ecology Progress Series, 497: 25–38, doi: 10.3354/meps10583

Nejstgaard J C, Båmstedt U, Bagøien E, et al. 1995. Algal constraints on copepod grazing. Growth state, toxicity, cell size, and season as regulating factors. ICES Journal of Marine Science, 52: 347–357

Parsons T R, Maita Y, Lalli C M. 1984. A Manual of Chemical and Biological Methods for Seawater Analysis. New York: Pergamon Press, 22–25

Platt T, Silvert W. 1981. Ecology, physiology, allometry and dimensionality. Journal of Theoretical Biology, 93: 855–860, doi: 10.1016/0022-5193(81)90343-X

Polovina J J, Woodworth P A. 2012. Declines in phytoplankton cell size in the subtropical oceans estimated from satellite remotely-sensed temperature and chlorophyll, 1998-2007. Deep-Sea Research: Part II. Topical Studies in Oceanography, 77-80: 82–88, doi: 10.1016/j.dsr2.2012.04.006

Qiu Dajun, Huang Liangmin, Zhang Jianlin, et al. 2010. Phytoplankton dynamics in and near the highly eutrophic Pearl River estuary, South China Sea. Continental Shelf Research, 30: 177–186, doi: 10.1016/j.csr.2009.10.015

Riegman R, Kuipers B R, Noordeloos A A M, et al. 1993. Size-differential control of phytoplankton and the structure of plankton communities. Netherlands Journal of Sea Research, 31: 255–265, doi: 10.1016/0077-7579(93)90026-O

State Oceanic Administration. 2008. GB 12763.4–2007 Specifications for Oceanographic Survey: Part 4. Survey of Chemical Parameters in Sea Water (in Chinese). Beijing: China Standard Press.

Song Shuqun, Sun Jun, Luan Qingshan, et al. 2008. Size-fractionated phytoplankton biomass in autumn of the Changjiang (Yangtze) River Estuary and its adjacent waters after the Three Gorges Dam construction. Chinese Journal of Oceanology and Limnology, 26(3): 268–275, doi: 10.1007/s00343-008-0268-0

Tamigneaux E, Legendre L, Klein B, et al. 1999. Seasonal dynamics and potential fate of size-fractionated phytoplankton in a temperate nearshore environment (Western Gulf of St Lawrence, Canada). Estuarine, Coastal and Shelf Science, 48: 253–269, doi: 10.1006/ecss.1999.0416

Tan Yehui, Huang Liangmin, Chen Qingchao, et al. 2004. Seasonal variation in zooplankton composition and grazing impact on phytoplankton standing stock in the Pearl River estuary, China. Continental Shelf Research, 24: 1949–1968, doi: 10.1016/j.csr.2004.06.018

Thomas C M, Perissinotto R, Kibirige I. 2005. Phytoplankton biomass and size structure in two South African eutrophic, temporarily open/closed estuaries. Estuarine, Coastal and Shelf Science, 65: 223–238, doi: 10.1016/j.ecss.2005.05.015

Utermöhl H. 1958. Zur Vervollkommnung der quantitativen Phytoplankton-Methodik. Mitteilungen der Internationale Vereinigung für Theoretische und Angewandte Limnologie, 9: 1–38

Uye S. 1986. Impact of copepod grazing on the red-tide flagellate *Chattonella antiqua*. Marine Biology, 92: 35–43, doi: 10.1007/BF00392743

Vollenweider R A, Giovanardi F, Montanari G, et al. 1998. Characterization of the trophic conditions of marine coastal waters with special reference to the NW Adriatic Sea: proposal for a trophic scale, turbidity and generalized water quality index. Environmetrics, 9: 329–357, doi: 10.1002/(ISSN)1099-095X

Wang Zhaoyu, Wang Jiangtao, Tan Liju. 2014. Variation in photosynthetic activity of phytoplankton during the spring algal blooms in the adjacent area of Changjiang River estuary. Ecological Indicators, 45: 465–473, doi: 10.1016/j.ecolind.2014.05.010

Yin Kedong, Zhang Jianlin, Qian Peiyuan, et al. 2004. Effect of wind events on phytoplankton blooms in the Pearl River estuary during summer. Continental Shelf Research, 24: 1909–1923, doi: 10.1016/j.csr.2004.06.015

Zhang J, Zhang Z F, Liu S M, et al. 1999. Human impacts on the large world rivers: would the Changjiang (Yangtze River) be an illustration?. Global Biogeochemical Cycles, 13: 1099–1105, doi: 10.1029/1999GB900044

Zhou Mingjiang, Shen Zhiliang, Yu Rencheng. 2008. Responses of a coastal phytoplankton community to increased nutrient input from the Changjiang (Yangtze) River. Continental Shelf Research, 28: 1483–1489, doi: 10.1016/j.csr.2007.02.009

Zhou Mingjiang, Yan Tian, Zou Jingzhong. 2003. Preliminary analysis of the characteristics of red tide areas in Changjiang River Estuary and its adjacent sea. Chinese Journal of Applied Ecology (in Chinese), 14: 1031–1038

Zhou Weihua, Yin Kedong, Long Aimin, et al. 2012. Spatial-temporal variability of total and size-fractionated phytoplankton biomass in the Yangtze River estuary and adjacent East China Sea coastal waters, China. Aquatic Ecosystem Health and Management, 15: 200–209, doi: 10.1080/14634988.2012.688727

Zhou Mingjiang, Zhu Mingyuan, Zhang Jing. 2001. Status of harmful algal blooms and related research activities in China. Chinese Bulletin of Life Sciences (in Chinese), 13(2): 54–59, 53